# WIND TUNNEL TEST RESULTS OF A NEW LEADING EDGE FLAP DESIGN FOR HIGHLY SWEPT WINGS - A VORTEX FLAP

L. James Runyan, Wilbur D. Middleton, and John A. Paulson,
Boeing Commercial Airplane Company

## SUMMARY

A new leading edge flap design for highly swept wings, called a vortex flap, has been tested on an arrow wing model in a low speed wind tunnel. A vortex flap differs from a conventional plain flap in that it has a leading edge tab which is counterdeflected from the main portion of the flap. This results in intentional separation at the flap leading edge, causing a vortex to form and lie on the flap. By "trapping" this vortex, the vortex flap can result in significantly improved wing flow characteristics relative to conventional flaps at moderate to high angles of attack, as demonstrated by the flow visualization results of this test.

## INTRODUCTION

At high angles of attack, highly swept, low aspect ratio wings develop a strong leading edge separation vortex (refs. 1-3). At a given angle of attack, this vortex results in an increase in lift, but an even larger increase in drag, thereby reducing L/D. Pitchup results due to the shift of lift inboard and toward the leading edge (ref. 4).

The usual method of preventing or delaying leading edge separation is to employ leading edge flaps, hinged panels deflected downward (refs. 5 and 6). A proposed alternate solution (see figure 1) is to induce and control separation on the deflected leading edge flap by use of a counterdeflected vortex flap extending from the leading edge of the main flap. The result is a "dog-leg" type flap on which a vortex is trapped. The low pressures associated with this trapped vortex act on the forward facing surface of the main flap, resulting in a thrust and, thereby, reducing drag. In addition, the trapped vortex gives the appearance of a large-radius leading edge to the outer flow. This makes it easier for the outer flow to attach at the knee of the flap and over the remainder of the wing, helping to reduce drag and control pitchup.

In this paper the results of a flow visualization test of the vortex flap on an arrow wing model are presented. Several different vortex flap configurations were tested at angles of attack ranging from $0^{\circ}$ to $20^{\circ}$. The flow visualization techniques included fluorescent oil, tufts, and a photographic wake pressure survey. The vortex flap results are compared to those of the basic arrow wing without flaps and to those with plain flaps.

## SYMBOLS

| | |
|---|---|
| b | wing span |
| $C_p$ | pressure coefficient |
| L | length |
| MS | model station |
| P | pressure |
| q | dynamic velocity |
| WBL | wing buttock line |
| V | velocity |
| y | distance along the span |
| $\alpha$ | angle of attack |
| $\delta$ | deflection angle |
| $\eta$ | normalized distance along span (y/b/2) |

Subscripts:

| | |
|---|---|
| F | flap |
| LE | leading edge |
| T | tab |
| o | total |
| $\infty$ | remote, undisturbed conditions |
| $\perp$ | normal to wing leading edge |

## WIND TUNNEL DESCRIPTION AND MODEL GEOMETRY

### Wind Tunnel

This test was performed in a Boeing low speed closed-circuit wind tunnel having a test section size of 36.6 cm by 45.7 cm. The Reynolds number for this test was about $2 \times 10^5$ based on the average model chord of 15.2 cm. The low Reynolds number should not have a significant effect on the vortex

flap results, because in all cases the leading edge of the flap is sharp, causing flow separation at that point. Also, based on results for similar flaps at higher Reynolds numbers (ref. 5), the plain flap results would not be expected to change significantly at higher Reynolds numbers.

## Model and Flaps

The arrow wing half model tested is shown in figure 2. It has a leading edge sweep of 67.2° and consists of a flat plate with sharpened leading and trailing edges. A fence on the inboard portion of the model near the wall prevented wind tunnel boundary layer air from being drawn onto the wing. Angle of attack was varied from 0° to 20°.

Figure 3 shows the leading edge flap configurations tested. One plain flap, two vortex flaps, a hybrid flap (plain flap inboard, vortex flap outboard), and a leading edge split flap were tested.

## Flow Visualization Techniques

The visual flow techniques used in this test were: fluorescent oil and mini-tufts to define the surface flow characteristics, streamers and smoke to reveal the flow field around the wing, and a wake survey technique which photographically maps the wake pressure just downstream of the wing.

Surface flow characteristics were made evident using fluorescent oil and tufts on separate runs. The tufts were very fine (0.0018 cm monofilament nylon), trimmed to a length of about 0.64 cm. Streamers 10 to 25 cm in length, of the same thread used for tufts, were also fixed in the incoming flow near the leading edge. Since the aerodynamic forces on these streamers are very low, streamlines can be approximated where the flow is steady. Smoke generated by heating kerosene was introduced in the wind tunnel inlet and illuminated as it passed over the model using a slit of light. With separated flow, the separation boundaries can be defined with this technique. Streamers caught in a vortex will also follow the separation boundary if properly positioned.

The wake pressures downstream of the model were mapped photographically, using the test apparatus illustrated in figure 4. A total pressure tube is mounted on the end of an arm which allows both vertical and radial motion in a plane approximately 1 cm downstream of the most aft point of the wing trailing edge. The pitot tube is traversed through the wing flow field in a series of radial arcs, each having a small vertical displacement from the preceding one. Pressure measured by the pitot tube, which is referenced to freestream static pressure, is sensed by a transducer, and the output from the transducer is fed through a voltage amplifier and filter into a signal splitter, which has several output circuits. Only one output circuit is activated at any given instant, corresponding to a specific voltage range on the incoming signal. The limits of each range can be adjusted, with no overlap. Two diodes, red and green, mounted on the traversing arm, each respond to one of these circuits. In the present test, the circuit to which the green diode was

connected was set to activate over the pressure range ($P_0 - P_\infty$) from 50% to 90% of freestream q. A camera placed in front of the diodes with the lens in the open position recorded an inverted picture of the wing wake, as shown in the left hand side of figure 5. A typical vortex has a green outer band, a red inner band, and a "black hole" in the center of the red band. Yellow bands occur in regions of high turbulence near the cross-over pressure level which result in rapid flickering of the red and green diodes, which the camera superimposes and sees as yellow. The amount of yellow in the pictures can be controlled, to a large extent, by filtering out the high frequency components of the signal.

## LEADING EDGE VORTEX CHARACTERISTICS

To assist in the interpretation of the oil flow photographs, the following description of leading edge vortex characteristics is given.

At angle of attack the flow separates from the leading edge of slender wings, creating vortex sheets which roll up to form a primary vortex on the suction side of the wing, as shown in figure 6a. The primary vortex rolls up above the wing and entrains additional airflow over the leading edge ahead of the aft attachment line. Inboard of this attachment line the upper surface flow is principally streamwise, as shown in figure 6b.

Under the primary vortex, the flow is accelerated strongly toward the leading edge until it passes under the vortex core, after which it recompresses and separates (along the secondary separation line). In the oil flow photographs, this area is seen as a series of scrubbed lines on the wing surface, which turn spanwise along the secondary separation line.

Forward of the secondary separation line, in the case of fully developed vortex flow, a secondary vortex is formed, rotating counter to the primary vortex. The secondary vortex, which is approximately 20 percent as strong as the primary vortex, looks like a zone of thick boundary layer in the photographs because it accumulates oil. Flow passing over the secondary vortex reattaches forward of the secondary vortex and continues to the leading edge where it separates again to join the primary vortex.

When the primary vortex moves off the wing trailing edge, the secondary vortex collapses to the trailing edge at the line of secondary separation. The wing tip flow outboard then consists of inboard reattached flow expanding to fill in under a "roof" formed by the lower layer of outboard wing leading edge separation. Depending upon the degree of expansion required and resultant recompression, the wing tip flow may remain attached or it may separate.

Figure 6c shows typical total pressure isobar patterns in the wake downstream of a highly swept wing with leading edge vortices. The vortices result in roughly circular low pressure isobar patterns above the outboard regions of the wing.

## RESULTS AND DISCUSSION

### Basic Arrow Wing

The flow characteristics of the basic arrow wing with no flaps are shown in figure 7. Oil flow and wake survey photographs at angles of attack of $5^{o}$, $10^{o}$, and $15^{o}$ are shown. At $\alpha = 5^{o}$, there is a small vortex that can be seen in the oil flow to originate at about 70 percent span. In the wake pressure survey this shows up as a small red area at the tip.

The oil flow photograph at $\alpha = 10^{o}$ shows that the primary vortex has increased in size and moved inboard. A secondary vortex can also be seen just outboard of the primary vortex. The wake pressure survey at $\alpha = 10^{o}$ shows the primary vortex as the large red area near the tip surrounded by the green and yellow band. The secondary vortex is the smaller red circular region just outboard of the primary vortex. The third (and smallest) red area nearest the wing tip is the tip vortex.

At $\alpha = 15^{o}$ the oil flow photo shows that the primary and secondary vortices now dominate the outboard half of the wing. The wake pressure survey shows that, downstream of the wing trailing edge, the primary and secondary vortices have begun to merge.

### Plain $50^{o}$ Flap

Oil flow results on the upper surface of the arrow wing with a $50^{o}$ leading edge plain flap are shown in figure 8. A vortex begins to develop at $\alpha = 5^{o}$, becoming larger and moving inboard as angle of attack is increased. The separation evident at the flap shoulder at this low Reynolds number would probably not change by a significant amount at higher Reynolds numbers.

Smoke flow was used to illuminate the dividing streamline characteristics of the plain flap, using the wind tunnel instrumentation illustrated in figure 9. A slit of light from a source mounted outside a window in the side of the test section impinges on smoke flowing over the wing leading edge, which is then photographed to produce a cross-sectional view of the flow.

The dividing streamline characteristics of the plain flap at $\alpha = 10^{o}$, as shown by smoke flow photographs, are shown in figure 10. Smoke introduced ahead of the wing reveals the exterior flow. If the smoke plume is moved inboard, the smoke is entrained inside the separation vortex. In both cases, the boundary between exterior flow and the interior (separated vortex) flow is defined. At $\eta = .80$ the flow can be seen to separate at the knee of the flap and reattach a short distance downsteam. At $\eta = .98$ the chordwise extent of separation is larger than at $\eta = .80$.

## 50° Vortex Flap

Figure 11 shows the results for the 50° vortex flap. At $\alpha = 10^{\circ}$ the oil flow photograph shows the flow to be attached over most of the wing upper surface, although the flow in the boundary layer is largely spanwise. A weak primary vortex subtends the flap from leading edge to the flap/wing corner, becoming stronger near the wing tip. The wake survey photos show both this primary vortex and a smaller vortex outboard resulting from the merging of the secondary and tip vortices. The improved flow over the surface and the reduced vortex size indicate a lower drag for this configuration than for the basic arrow wing with no flaps. Thus, it appears that the 50° vortex flap is performing well at $\alpha = 10^{\circ}$.

At $\alpha = 15^{\circ}$, the 50° vortex flap results in a small reduction in the size of the primary vortex (compared to the basic wing). The secondary separation line inboard lies near the leading edge wing/flap break, trailing back behind the flap at about 40 percent span. Outboard, the secondary vortex (which is separate from the primary in the wake photograph) moves from the flap onto the wing surface and the flow separates from the flap at about 90% span. The vortex flap may still be somewhat effective at reducing drag at this condition.

The upper surface flow characteristics at 10° angle of attack of the basic wing, the 50° plain flap, and the 50° vortex flap are compared in figure 12. It can be seen that only the 50° vortex flap shows no sign of a vortex on the wing.

Smoke patterns for the 50° vortex flap, shown in figure 13, show that the trapped vortex on the vortex flap gives the wing the appearance of having a large leading-edge radius with attached upper surface flow, except for the tip region. At $\eta = .80$, it can be seen that the vortex flap is successful in preventing separation at the wing-flap junction. A relatively thick boundary layer appears to remain, however. This is further illustrated by the streamer shown in two views in figure 14. The streamer was located as close to the wing surface as possible for stability. Note the strong shear indicated by direction of the tufts compared to the streamer. The streamer could not be located this close to the wing with plain flaps.

## Variable Deflection Vortex Flap

A variable deflection vortex flap was designed so that the local deflection angle of the main flap would nominally match the local angle of attack for a wing angle of attack of 8°. The resulting deflection angle varied from 16° at the root to 76° at the tip, with the tab bent back parallel to the wing plane.

Results for the variable deflection vortex flap are shown in figure 15. At $\alpha = 5^{\circ}$, a primary vortex appears to subtend the flap out to approximately 60 percent span, with the aft attachment line near the flap/wing corner. The flap appears ineffective at $\alpha = 10^{\circ}$ and greater. The flow at $\alpha = 10^{\circ}$ looks much like the 50° vortex flap at $\alpha = 15^{\circ}$. At $\alpha = 15^{\circ}$, the flow

outboard of approximately 40 percent span is separated and eddying with a secondary vortex near the secondary separation line on the main wing surface. The vortex size in the wake photographs is approximately the same as for the basic wing. (The extensive regions of yellow coloration in figure 15 resulted from the use of a different transducer signal filter setting than was used for figures 7 and 11. The overall size of the vortex as seen by the camera is not appreciably affected by the filter setting, however.)

### Hybrid Flap

Another alternative to the 50° vortex flap was a hybrid arrangment, consisting of a 30° plain flap on the inboard 25% of the wing span, a vortex flap having a deflection angle varying from 30° inboard to 50° outboard extending from 25% span to 50% span, and a 50° vortex flap on the outboard 50% of the wing. The philosophy of the plain flap inboard was to postpone intentional tripping of the vortex to a more outboard location, thereby resulting in a weaker primary vortex at the tip. The oil flow photo at $\alpha = 10^{\circ}$ in figure 16 shows a small separation bubble at the hinge of the 30° plain flap, with subsequent flow reattachment. The size of the vortex near the wing tip at $\alpha = 10^{\circ}$ is about the same as that of the 50° vortex flap. There are also two small vortices near the mid-span location which trail back from the junctions of the flap segments. At $\alpha = 15^{\circ}$, the flow characteristics for the hybrid flap are very similar to the 50° vortex flap.

### Leading Edge Split Flap

The leading edge split flap had a constant deflection of 45° along the entire span and an increased flap chord (1.8 cm). The junction of the wing and flap was 0.5 cm behind the rounded leading edge. The flow characteristics resulting from this flap configuration, as shown in figure 17, exhibit strong secondary vortex flow. At $\alpha = 15^{\circ}$, it has a significantly smaller primary vortex than all others tested. Since it is a design goal to have a flap design which works well on the arrow wing at $\alpha = 15^{\circ}$, further investigation of the leading edge split flap concept is planned.

## CONCLUDING REMARKS

Flow visualization tests of an arrow wing model in a Boeing low speed wind tunnel have shown promising results for vortex flaps. These results indicate that the vortex flap is able to "trap" the leading edge separation vortex on its surface at angles of attack up to 10°. The "trapped" vortex gives the appearance of a large radius leading edge to the outer flow. As a result, no flow separation at the wing-flap junction was observed for angles of attack up to 10°. A hybrid flap configuration consisting of a plain flap inboard and a vortex flap outboard was also successful in improving the upper surface flow characteristics at $\alpha = 10^{\circ}$. Optimization of the vortex flap geometry parameters should result in additional improvements in the performance of the vortex flap.

## REFERENCES


1. Stanbrook, A., and Squire, L. C.: Possible Types of Flow at Swept Leading Edges, The Aeronautical Quarterly, pp 77-82, February 1967

2. Kulfan, R. M.: Wing Airfoil Shape Effects on the Development of Leading Edge Vortices, AIAA Paper No. 79-1675, Presented at the AIAA Atmospheric Flight Mechanics Conference, Boulder, Colorado, August 7, 1979

3. Kulfan, R. M.: Wing Geometry Effects on Leading Edge Vortices, AIAA Paper No. 79-1872,, Presented at the AIAA Aircraft Systems and Technology Meeting, New York, New York, August 20-22, 1979

4. Chambers, Joseph R.: Aerodynamic Characteristics at High Angles of Attack, Paper Presented at the AGARD/VKI Lecture Series on "Aerodynamic Inputs for Problems in Aircraft Dynamics", Rhode-St-Genese, Belgium, April 25-29, 1977

5. Coe, Paul L. and Weston, Robert P.: Effects of Wing Leading-Edge Deflection on the Low-Speed Aerodynamic Characteristics of a Low-Aspect-Ratio Highly Swept Arrow-Wing Configuration. NASA Technical Memorandum 78787, September 1978

6. Coe, Paul L. and Huffman, Jarrett K.: Influence of Optimized Leading-Edge Deflection and Geometric Anhedral on the Low-Speed Aerodynamic Characteristics of a Low-Aspect-Ratio Highly Swept Arrow-Wing Configuration, NASA TM-80083, June 1979

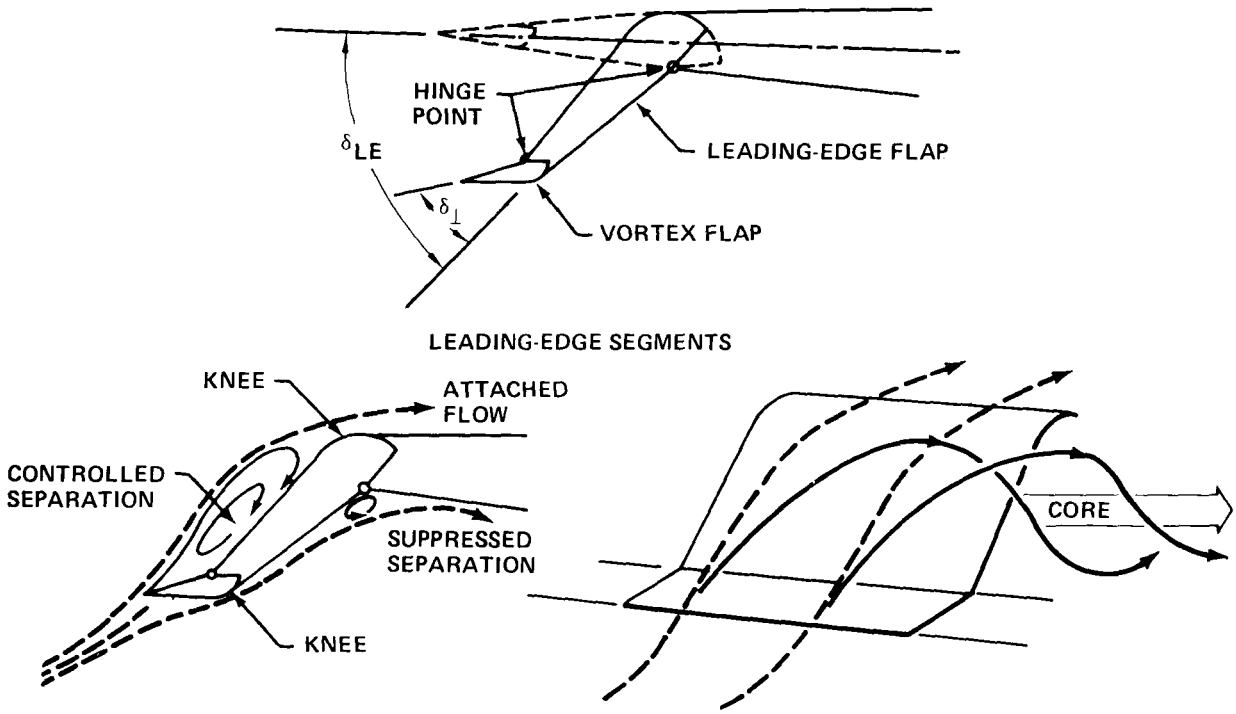


Figure 1.- Vortex control flaps.

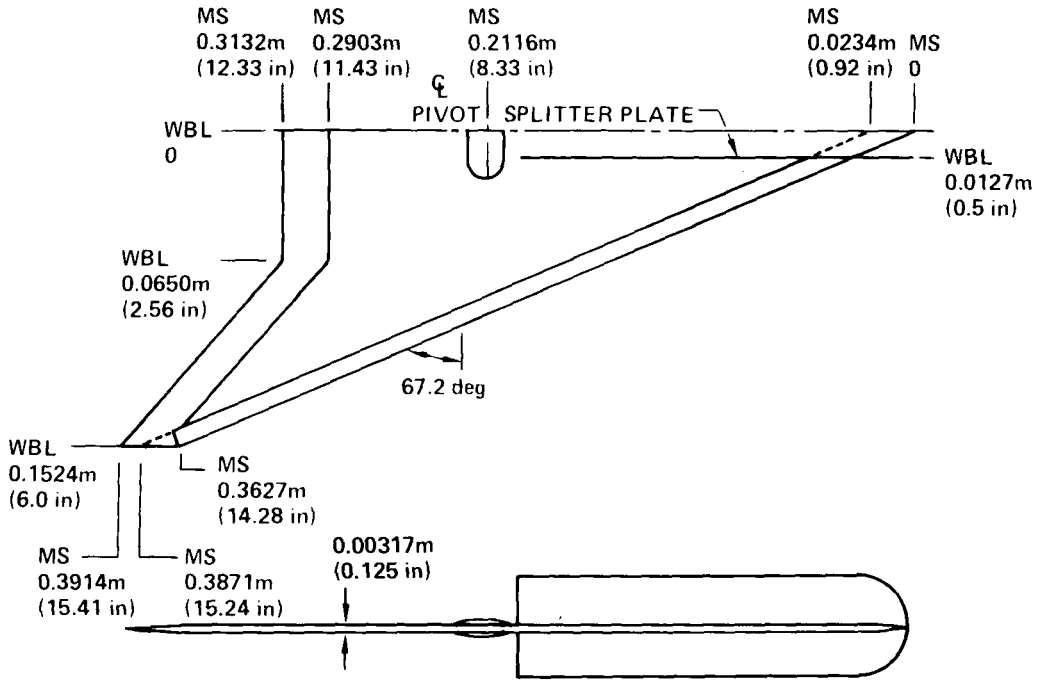


Figure 2.- Arrow wing model geometry.

● ANGLES MEASURED NORMAL TO LEADING EDGE

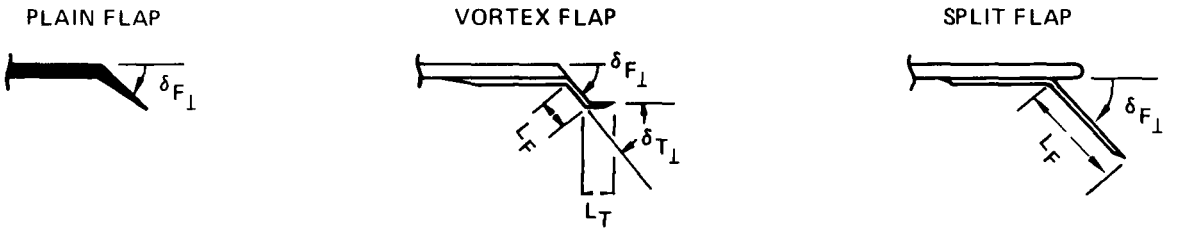


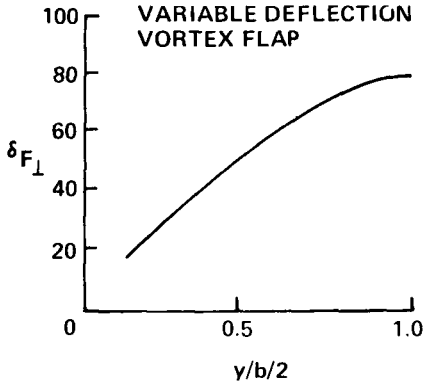


| FLAP DESIGNATION | $\delta_{F_\perp}$ | $L_F$ | $\delta_{T_\perp}$ | $L_T$ |
|---|---|---|---|---|
| PLAIN FLAP | 50 deg | 0.00890m (0.35 in) | — | — |
| 50-deg VORTEX FLAP | 50 deg | 0.00445m (0.175 in) | -50 deg | 0.00445m (0.175 in) |
| VARIABLE DEFLECTION VORTEX FLAP | SEE PLOT ON LEFT | 0.00445m (0.175 in) | $-\delta_{F_\perp}$ | 0.00445m (0.175 in) |
| HYBRID FLAP | 30-deg PLAIN FLAP ON INBOARD 25% OF SPAN; VORTEX FLAP VARYING FROM $\delta_{F_\perp}$ = 30 deg AT 25% SPAN TO $\delta_{F_\perp}$ = 50 deg FROM 50% SPAN TO TIP | | | |
| LEADING EDGE SPLIT FLAP | 45 deg | 0.0178m (0.7 in) | — | — |

Figure 3.- Flap geometry.

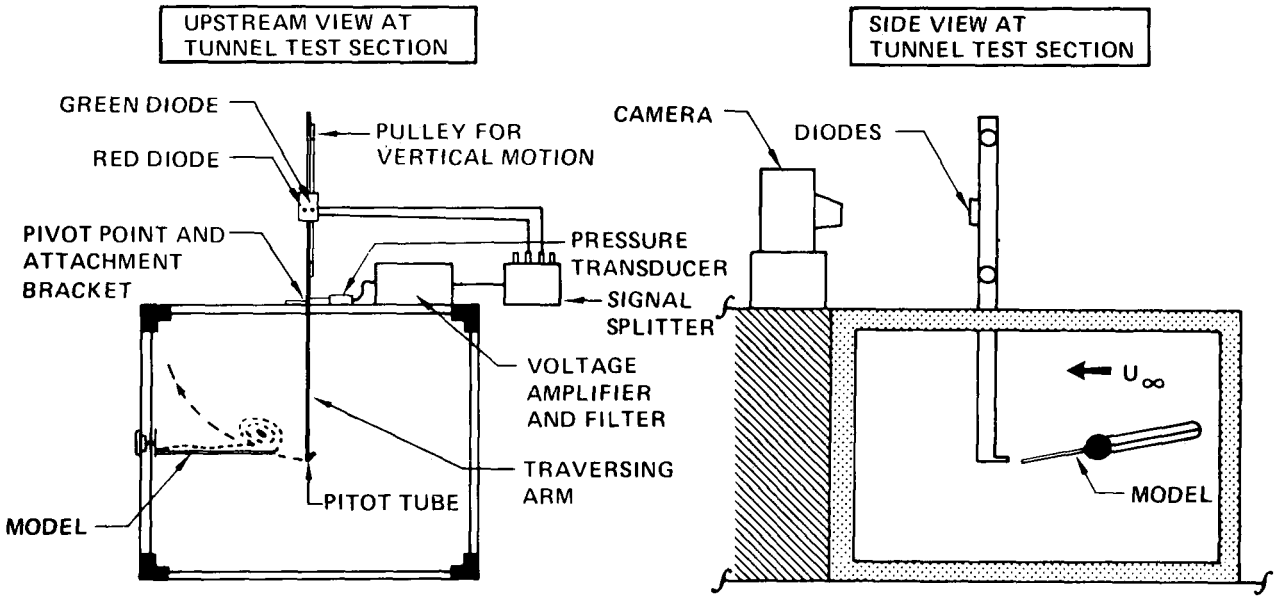


Figure 4.- Wake pressure survey apparatus.

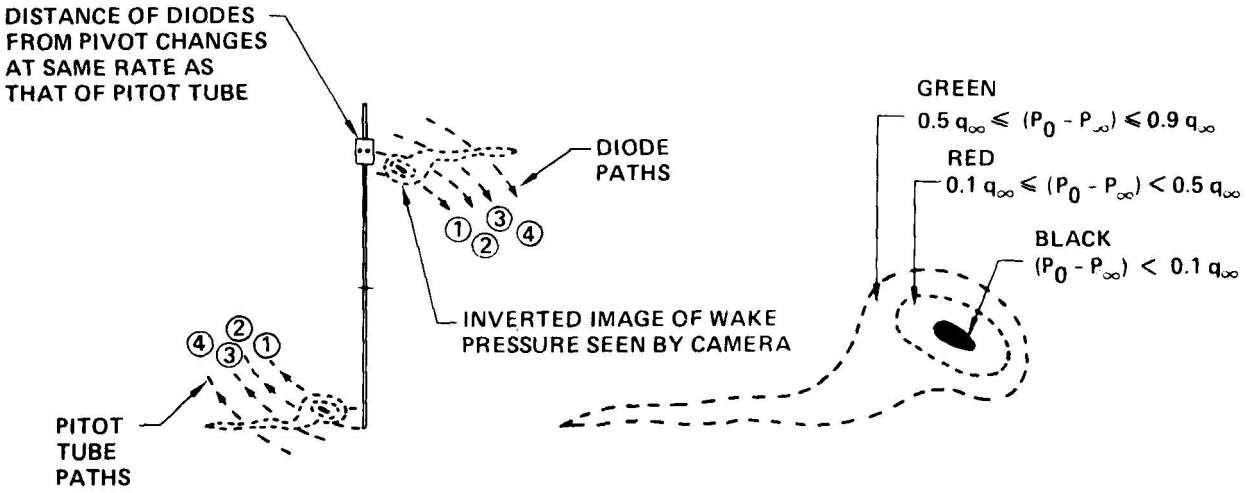


Figure 5.- Wake pressure survey technique.

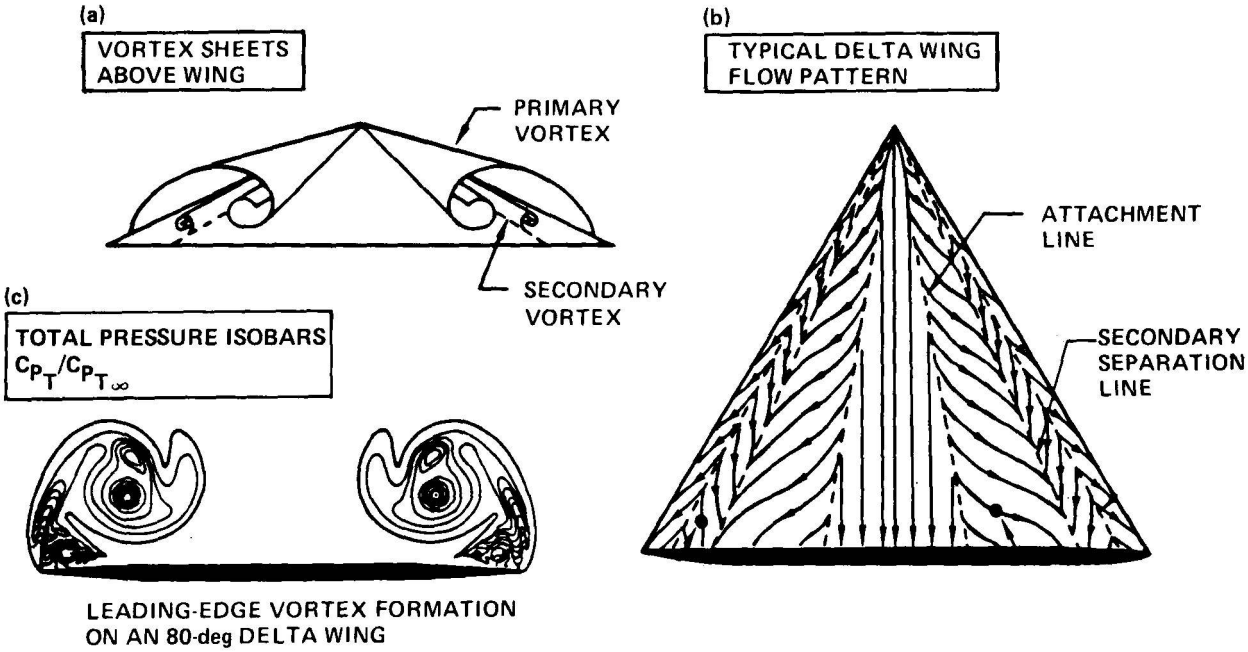


Figure 6.- Vortex flow characteristics.

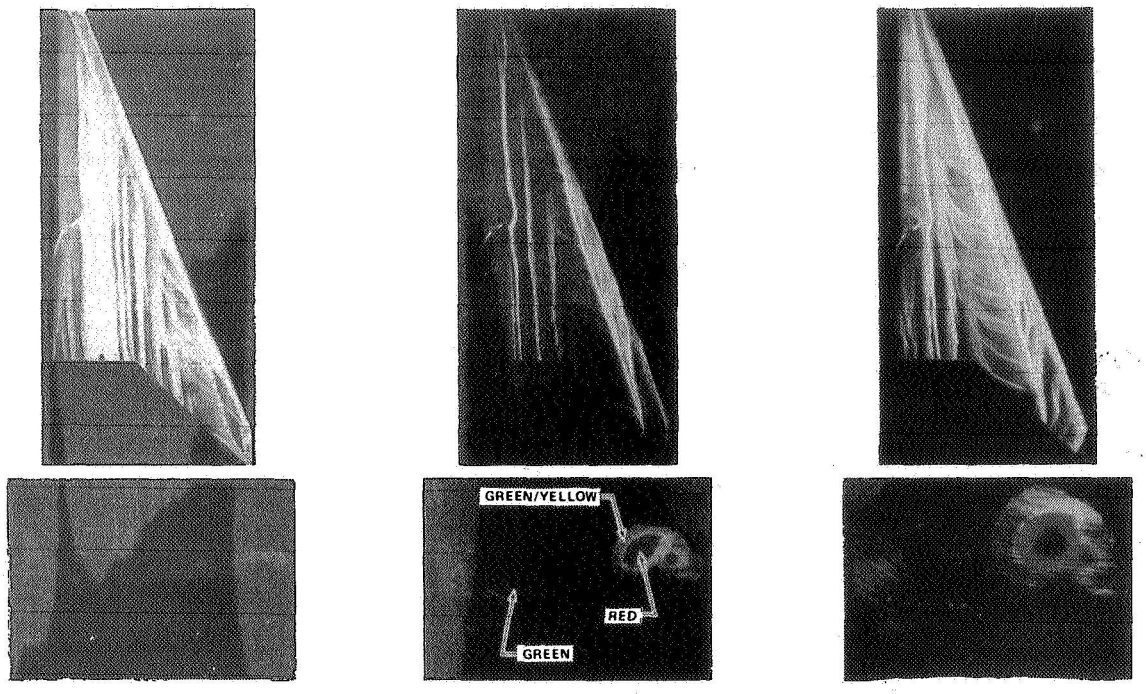


Figure 7.- Oil flow and wake survey of basic arrow wing.

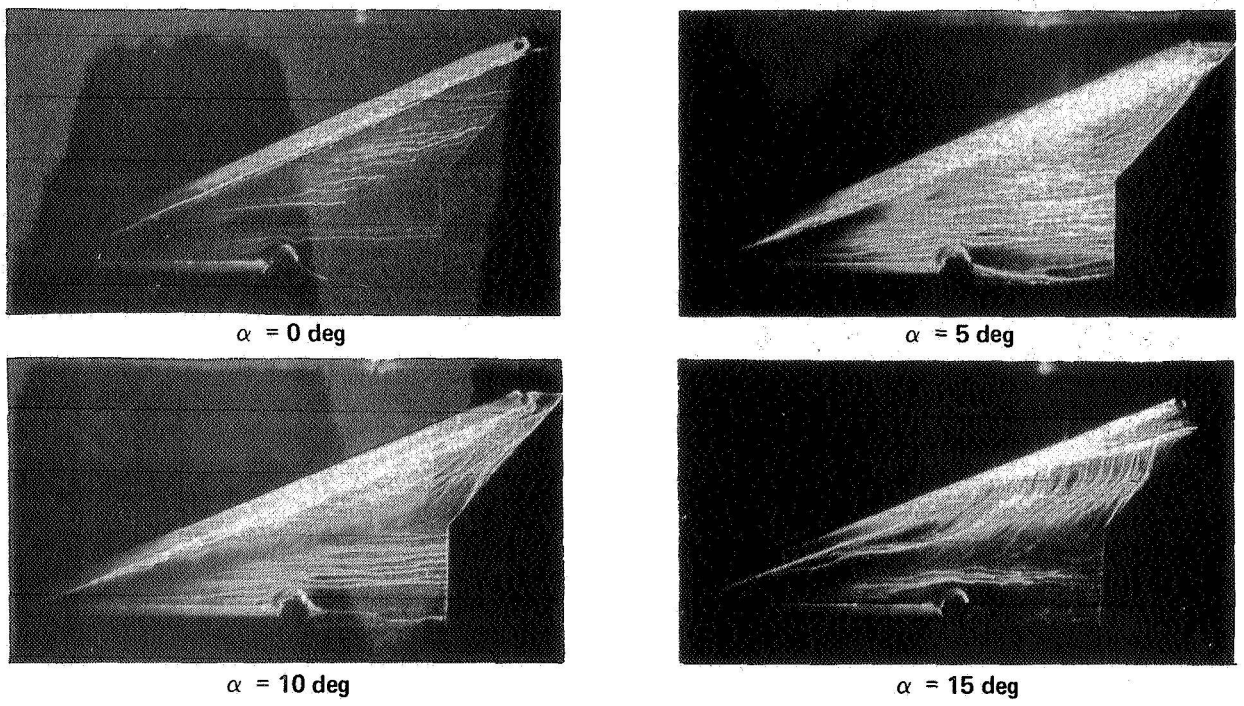


Figure 8.- Oil flow for 50° plain flap.

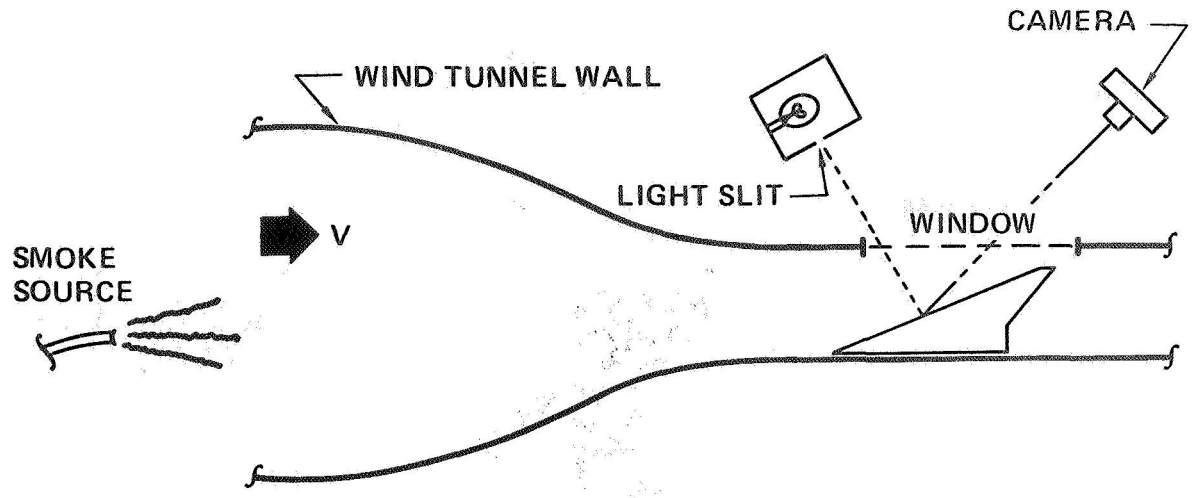


Figure 9.- Wind tunnel instrumentation for dividing streamline photographs.

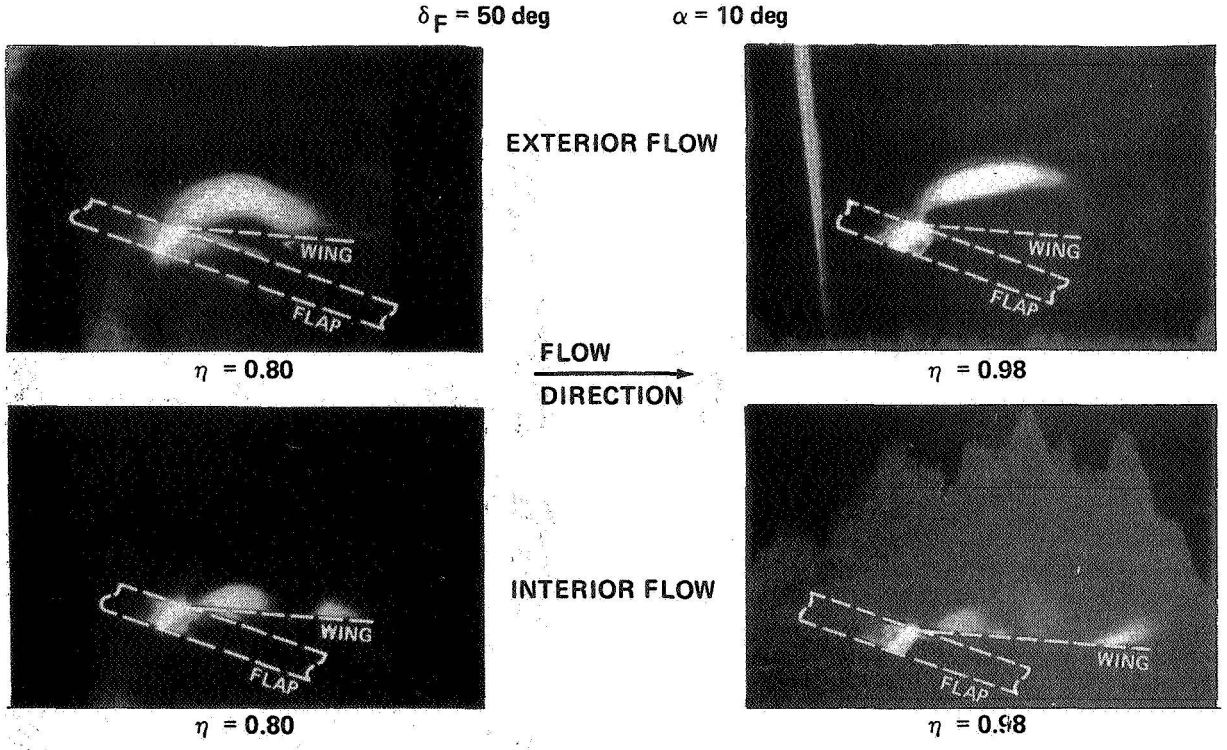


Figure 10.- Dividing streamline characteristics for 50° plain flap.

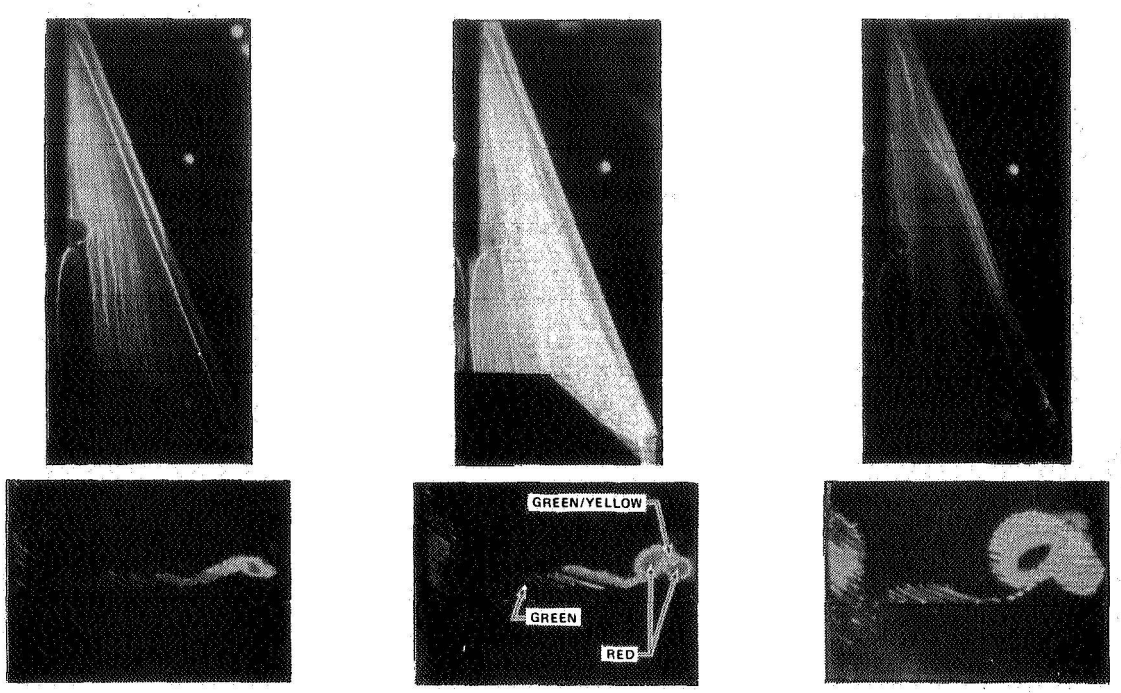


Figure 11.- Oil flow and wake survey for 50° vortex flap.

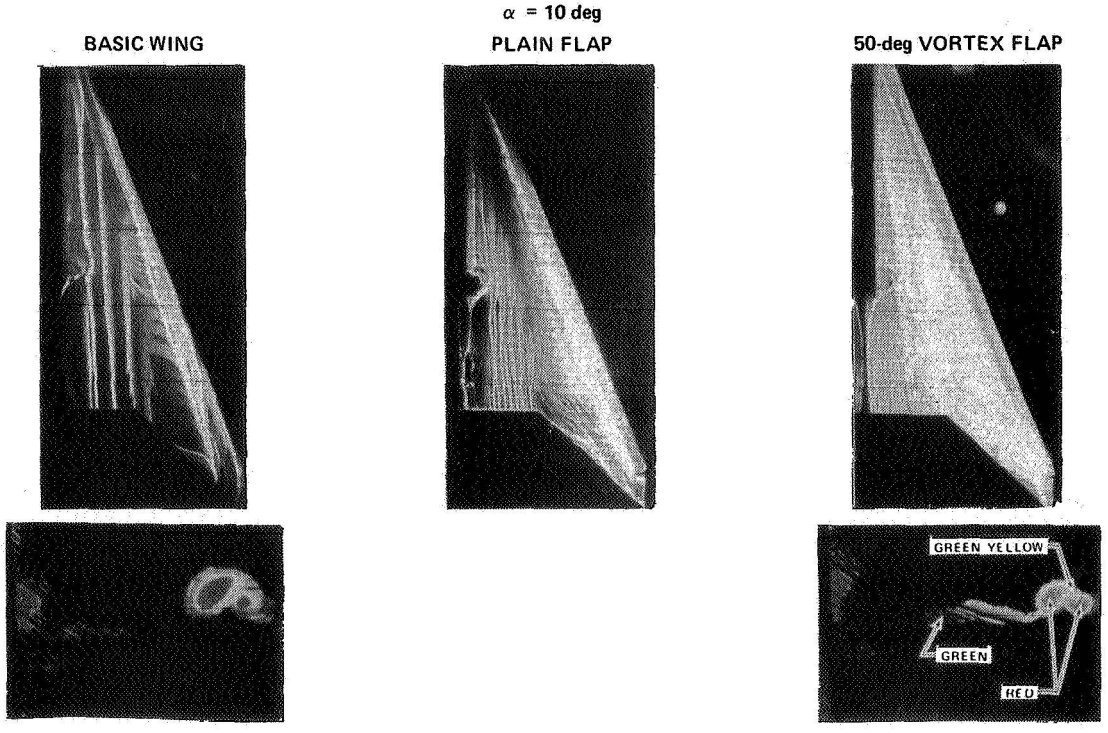


Figure 12.- Comparison of basic wing, plain flap, and 50° vortex flap.

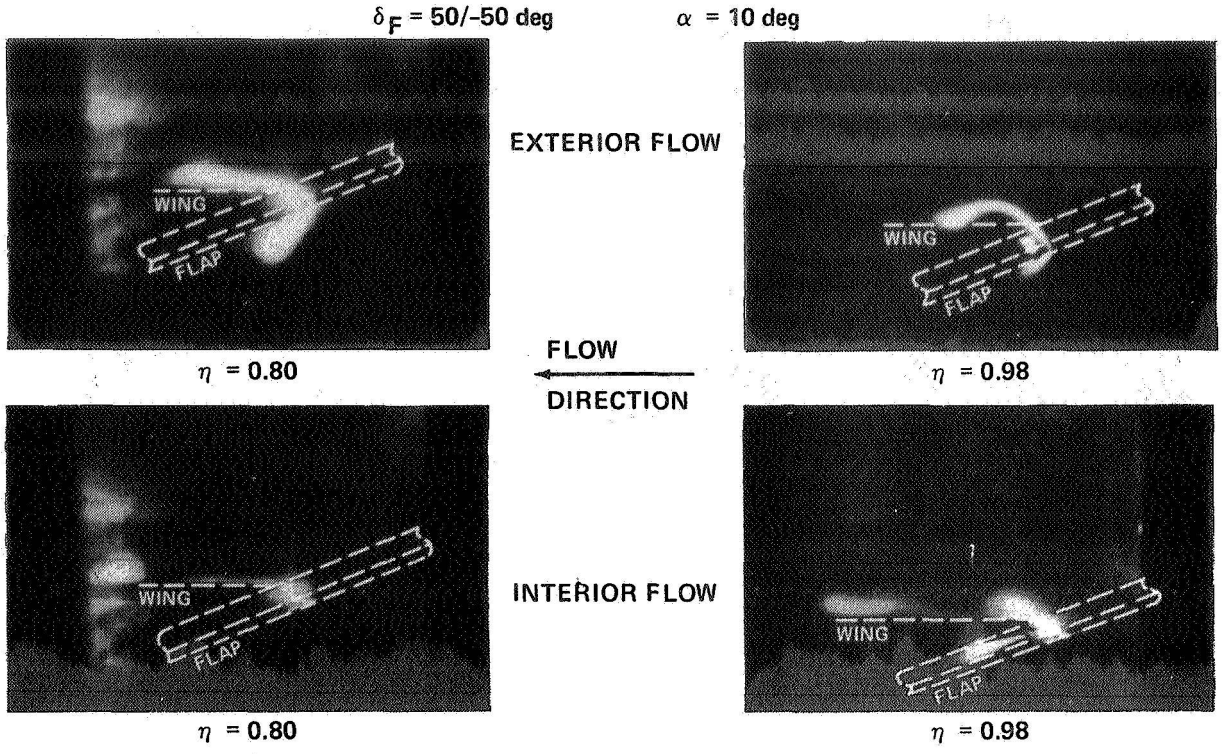


Figure 13.- Dividing streamline characteristics for 50° vortex flap.

$\alpha$ = 10 deg $\eta$ = 0.80

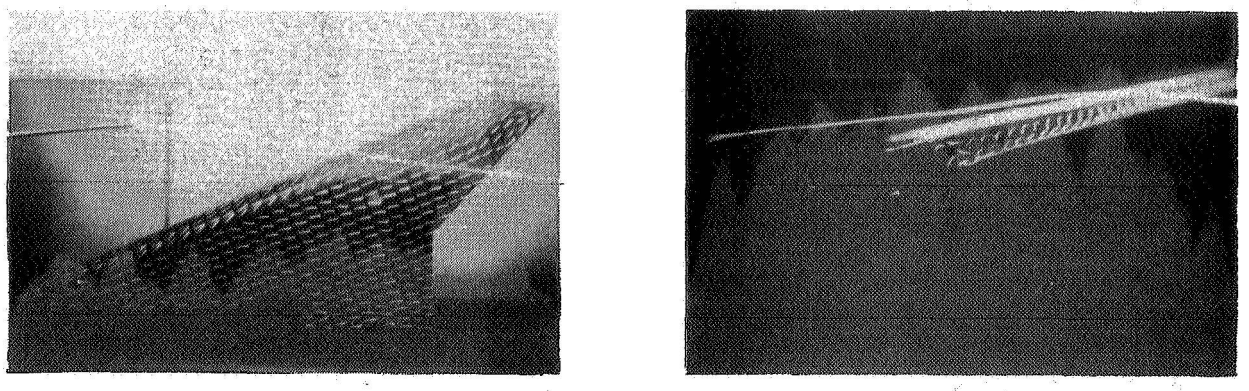

Figure 14.- Streamer above arrow wing with 50° vortex flap.

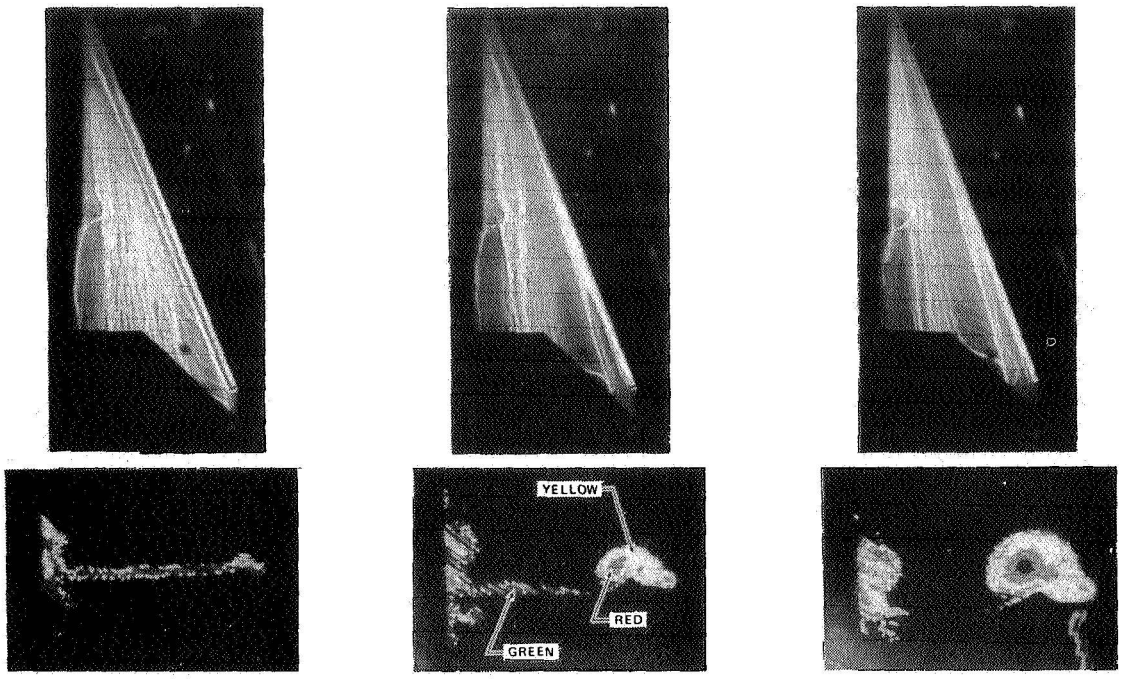


α = 5 deg  α = 10 deg  α = 15 deg

Figure 15.- Oil flow and wake survey for varying deflection vortex flap.

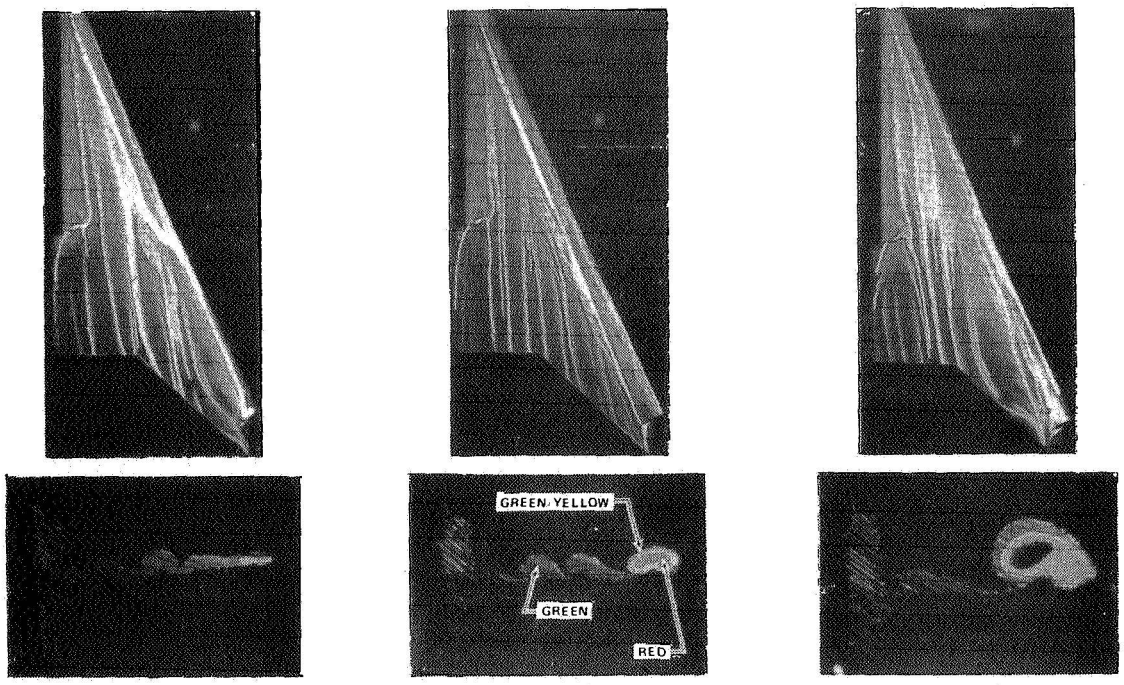


α = 5 deg  α = 10 deg  α = 15 deg

Figure 16.- Oil flow and wake survey for hybrid flap.

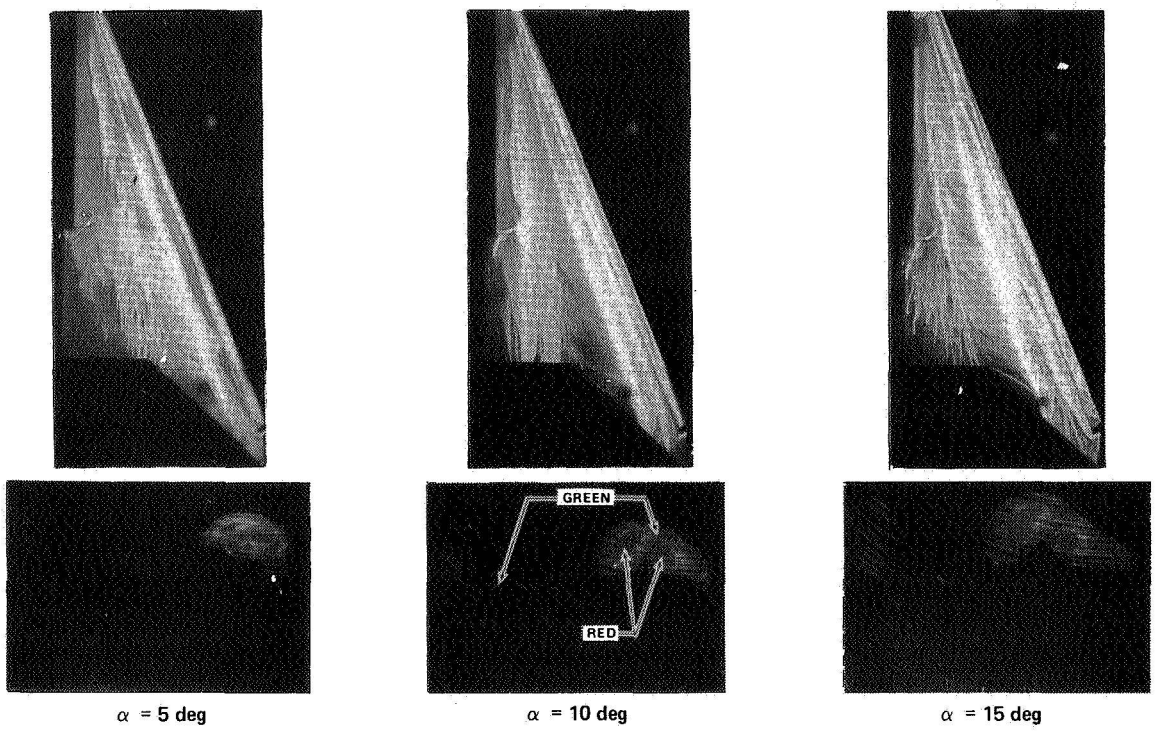


Figure 17.- Oil flow and wake survey for 45° leading-edge split flap.